



INSTITUT DE FRANCE  
Académie des sciences

# *Comptes Rendus*

---

## *Mécanique*

Ahmed Maati, El Hadj Ouakdi, Laurent Tabourot and Pascale Balland

**A contribution to the modelling of creep behaviour of FCC metals**

Volume 349, issue 1 (2021), p. 55-64

Published online: 4 March 2021

<https://doi.org/10.5802/crmeca.76>



This article is licensed under the  
CREATIVE COMMONS ATTRIBUTION 4.0 INTERNATIONAL LICENSE.  
<http://creativecommons.org/licenses/by/4.0/>



*Les Comptes Rendus. Mécanique* sont membres du  
Centre Mersenne pour l'édition scientifique ouverte  
[www.centre-mersenne.org](http://www.centre-mersenne.org)  
e-ISSN : 1873-7234



---

Synthesis / Synthèse

# A contribution to the modelling of creep behaviour of FCC metals

Ahmed Maati<sup>\*</sup>, <sup>a, b</sup>, El Hadj Ouakdi<sup>b</sup>, Laurent Tabourot<sup>c</sup> and Pascale Balland<sup>c</sup>

<sup>a</sup> Mechanics Laboratory, Department of Mechanics, Amar Telidji University, Laghouat 03000, Algeria

<sup>b</sup> Laboratory of Physics and Mechanics of Metallic Materials, Setif 1 University, Setif 19000, Algeria

<sup>c</sup> SYMME Laboratory, Univ. Savoie Mont Blanc, FR-74000 Annecy, France

*E-mails:* a.maati@lagh-univ.dz (A. Maati), elouakdi@univ-setif.dz (E. H. Ouakdi), laurent.tabourot@univ-smb.fr (L. Tabourot), pascale.balland@univ-smb.fr (P. Balland)

**Abstract.** In this paper, a new modelling is proposed to describe the viscoplastic behaviour of face-centred cubic (FCC) metals. Creep tests under various conditions were performed. The material chosen to test the model is Al-1050. The plastic deformation is controlled by intragranular diffusion when the test temperature exceeds  $0.4T_m$ . The developed model involves two state variables related to the microstructure: dislocation density and subgrain size. The grain size is assumed to be constant in the intermediate temperature range. Validation tests were proposed to justify the reliability of the developed model in various loading conditions.

**Keywords.** Creep, Subgrain, Strain hardening, Dynamic recovery, Viscoplasticity, Intragranular diffusion.

*Manuscript received 24th October 2020, revised 27th December 2020, accepted 1st February 2021.*

## 1. Introduction

The development of forming operations of sheet metal requires the use of numerical simulation tools based on the resolution methods such as finite element methods. For this purpose, the choice of the accurate modelling of thermomechanical behaviour of the material that has to be introduced in the numerical code is a decisive step. Various models are now available in the literature to describe at low scale the viscoplastic behaviour by taking into account inter- and intragranular effects (model of Pierce and *et al.* (1983), model of Cuitino Ortiz (1992), model of Teodosiu *et al.* (1997), etc.). The models are selected so that they present a similar formalism: a flow law plus a hardening law. This makes it possible to use the same numerical scheme to integrate each model [1]. In our case, a viscoplasticity model based on physics is proposed to describe the thermomechanical behaviour during creep tests of face-centred cubic (FCC) metals

---

\* Corresponding author.

such as Al-1050. Dislocations are important microstructure features, as their mobility greatly impacts the strength and plasticity of crystal materials [2]. Therefore, dislocations and their associated mechanisms for a given microstructure are generally self-sufficient to macroscopically explain most of the mechanical properties [3]. Physically, strain hardening and dislocation patterning are strongly interrelated. The microstructure evolution during high-temperature deformation is to be taken into account. Definitely, the temperature plays an important role in the development of microstructures by promoting the annihilation of dislocations and thus the dynamic recovery. The evolution of dislocation density and their structuring within the material controls the evolution of flow stress during the plastic deformation. To determine the effects of complex loading, it is wiser to use models whose state variables related to dislocations microstructure are better able to evolve according to the history of the material [4]. In this study, two internal state variables (dislocation density and subgrain size) under different loading conditions were investigated. It is important to note that the present article can be considered as an extension of a recently published study [5], the latter was devoted to modelling the thermomechanical behaviour of FCC metals (e.g. aluminium 1050A alloy) under tensile tests. All the tests were performed for each imposed temperature and a constant strain rate, the time factor is not taken into account. The effect of microstructure on the mechanical behaviour during plastic deformation was investigated. Two opposite and simultaneous physical phenomena were generated during plastic deformation: the strain hardening rules that occur because of dislocation multiplication mechanism within the crystal structure of the metal and the dynamic recovery governed by thermal activation. Dynamic recovery allows dislocations to overcome obstacles to their motion to form a cell structure more homogeneous and less dense [6]. The theory of thermal activation indicates that we will have to apply to the dislocation located at a point, a stress at least equal to the internal stress exerted on the dislocation ( $\sigma \approx \sigma_\mu$ ) [7]. In the intermediate temperature range ( $T \geq 0.4T_m$ ), the process of annihilation and rearrangement of dislocations may give rise to the formation of subgrains or dislocation cells, which contribute to the strength of the metal [8]. In this study, the evolution of internal stress and dislocation microstructures during creep tests under the coupling effect of strain rate and temperature was investigated. New equations were developed to predict the thermomechanical behaviour in creep for FCC metals under various conditions with and without sudden change in load. A set of constitutive equations and model parameters were used to describe the creep behaviour of FCC metals over a wide range of strain rate and temperature. Experimental data derived from literature [9] are used to validate numerical results.

## 2. Presentation of the thermomechanical model under tensile test

For temperatures higher than  $0.4T_m$ , the applied stress depending on the microstructural parameters is represented by the internal stress according to the following relationship [10]:

$$\sigma \approx \sigma_\mu(\varepsilon, \dot{\varepsilon}, T) = \alpha_1 G b \sqrt{\rho} + \alpha_2 G \sqrt{\frac{b}{d}} + \alpha_3 G \sqrt{\frac{b}{D}}, \quad (1)$$

where  $\alpha_1$ ,  $\alpha_2$ , and  $\alpha_3$  are dimensionless constants.

The microstructural parameters  $\rho$  and  $d$  vary significantly during plastic deformation and are closely dependant on strain rate and temperature [5]:

$$\rho = \rho_s (1 - K \exp(-K_a \varepsilon)) \quad (2)$$

$$d = d_s (1 + 2 \exp(-K'_a \varepsilon)) \quad (3)$$

**Table 1.** Numerical values of model constants [5]

$\alpha_1$	$\alpha_2$	$\alpha_3$	$d_{s0}$ ( $\mu\text{m}$ )	$n$	$B$ ( $m^{-2/5}$ )	$D$ ( $\mu\text{m}$ )	$A$ ( $m^{3/5} \times 10^{-6}$ )	$\rho_0$ ( $\mu\text{m}^{-2}$ )	$C$	$b$ ( $\mu\text{m}$ )
0.2	0.07	0.08	0.5	5.0	7500	60	2500	5.0	40	$2.86 \times 10^{-4}$

with

$$\rho_s(\dot{\epsilon}, T) = \left[ \frac{1}{bd_s K_a} \right] + \rho_0 \tag{4}$$

$$d_s(\dot{\epsilon}, T) = d_{s0} + A \left( \frac{\dot{\epsilon}}{D_L} \right)^{-\frac{1}{n}} \tag{5}$$

$$K_a(\dot{\epsilon}, T) = K_{a0} + B \left( \frac{\dot{\epsilon}}{D_L} \right)^{-\frac{1}{n}} \tag{6}$$

$$K'_a = C \cdot K_a \tag{7}$$

$$K = \frac{1}{1 + bd_s K_a \rho_0} \tag{8}$$

$$K_{a0} \approx 3d_{s0}, \tag{9}$$

where  $A, B, C$ , and  $n$  are constants determined from uniaxial tensile test.  $K$  is an integration constant.  $d_{s0}$  and  $K_{a0}$  represent, respectively, the values of  $d_s$  and  $K_a$  for low temperatures and/or high strain rates [11].  $\rho_0$  represents the dislocation density before deformation, we introduced this quantity in order to account properly the initial conditions of the deformation.

The diffusion coefficient  $D_L(T)$  is given by the following relation [12]:

$$D_L(T) = 1.7 \times 10^{-4} \exp\left(\frac{-142}{RT}\right) + 6 \times 10^{-7} \exp\left(\frac{-115}{RT}\right). \tag{10}$$

As a reminder, the basic equations (2) to (9) have been developed and demonstrated in the previous publication [5]. In addition, the constants of the model were identified in this step (Table 1). These values were chosen on the basis that they give a best fit of numerical curves to the experimental data.

### 3. Modelling of creep at constant load

The creep process is accompanied by many different microstructural rearrangements including dislocation movement, ageing of microstructure, and grain-boundary cavitation [13]. This phenomenon is highlighted by tensile test under constant load. The deformation occurs instantaneously and the behaviour is highly sensitive to strain rate  $\dot{\epsilon}$ . The test reveals the influence of temperature and applied load on the various stages of creep by taking into account the evolution of two internal parameters ( $\rho$  and  $d$ ). The creep curves can be represented in two types of function  $\epsilon(t)$  or  $\dot{\epsilon}(\epsilon)$ . For an irreversible deformation process, an incremental relationship involving stress, strain, and strain rate is defined as follows [9]:

$$d\sigma = \theta d\epsilon + \beta d \ln \left( \frac{\dot{\epsilon}}{D_L} \right) \tag{11}$$

with

$$\theta = \left( \frac{\partial \sigma}{\partial \epsilon} \right)_{(\dot{\epsilon}, T)}; \quad \beta = \left( \frac{\partial \sigma}{\partial \ln \left( \frac{\dot{\epsilon}}{D_L} \right)} \right)_{\epsilon}$$

$\theta$  and  $\beta$  are analytically calculated using the relationships previously described:

$$\theta = \frac{K_a \sigma_\rho}{2} \left[ \left( \frac{\sigma_{\rho s}}{\sigma_\rho} \right)^2 - 1 \right] + \frac{CK_a \sigma_{d_s}}{2} \left[ 1 - \left( \frac{\sigma_d}{\sigma_{d_s}} \right)^2 \right] \quad (12)$$

$$\beta = -\frac{1}{10d_s} \left\{ 2\sigma_s \left[ \frac{K_a \varepsilon}{2} \left\langle \left( \frac{\sigma_{\rho s}}{\sigma_\rho} \right)^2 - 1 \right\rangle - 1 \right] + \sigma_d \left[ K'_a \varepsilon \left\langle 1 - \left( \frac{\sigma_d}{\sigma_{d_s}} \right)^2 \right\rangle - 1 \right] \right\} \quad (13)$$

$\sigma_{\rho s}$  and  $\sigma_{d_s}$  are used to simplify the expressions of  $\theta$  and  $\beta$  such as

$$\sigma_{\rho s} = \alpha_1 G b \sqrt{\rho_s}; \quad \sigma_{d_s} = \alpha_2 G \sqrt{\frac{b}{d_s}}.$$

The flow stress evolution during creep can also be expressed in exponential form as a function of effective strain:

$$\sigma = \sigma_0 \exp(\varepsilon) \quad (14)$$

$\sigma_0$  is the initial stress corresponding to the beginning of primary stage of creep (at  $\varepsilon = 0$ ). It is deduced from (1) by using the minimum boundary condition:

$$\sigma_0 = \alpha_1 G b \sqrt{\rho_0} + \alpha_2 G \sqrt{\frac{b}{d_0}} + \alpha_3 G \sqrt{\frac{b}{D}}. \quad (15)$$

This study assumed that the metal does not undergo recrystallization of the structure, then the grain size remains constant ( $D = D_0 = \text{constant}$ ).

The viscoplastic behaviour expressed by the function  $\dot{\varepsilon}(\varepsilon)$  can therefore be formulated combining equations (1) and (15):

- Creep at constant load ( $d\sigma/d\varepsilon = \sigma$ ):

$$\frac{d\dot{\varepsilon}}{d\varepsilon} = \left( \frac{\sigma - \theta}{\beta} \right) \dot{\varepsilon} \quad (16)$$

- Creep at constant stress ( $d\sigma = 0$ ):

$$\frac{d\dot{\varepsilon}}{d\varepsilon} = \left( \frac{-\theta}{\beta} \right) \dot{\varepsilon}. \quad (17)$$

The numerical integration of relationships (13) and (14) allows us to plot the creep curves  $\dot{\varepsilon}(\varepsilon)$  at constant load and at constant stress, respectively. However, before making the numerical calculation, we must first find the initial values  $d_{si}$  and  $\dot{\varepsilon}_{0i}$  corresponding just at the beginning of the primary creep. The expression of  $d_{si}$  is obtained directly from the relationship (12).  $d_0$  is taken equal to 3 times the value of  $d_{si}$  [14, 15]:

$$d_{si} = \frac{\alpha_2^2 G^2 b}{3(\sigma_0 - \sigma_{\rho 0} - \sigma_D)^2}. \quad (18)$$

The expression of the initial strain rate ( $\dot{\varepsilon}_{0i}$ ) corresponding to subgrain size  $d_{si}$  can be determined from the relationship (2):

$$\dot{\varepsilon}_0 = \left( \frac{A}{d_{si} - d_{s0}} \right)^5 D_L. \quad (19)$$

To ensure the consistency of our model, several tests under various conditions were performed by comparing the calculated results with the experimental ones. A computer program (Fortran in our case) is used to plot numerical graphs from the different relationships of the model. Figure 1, for example, describes the creep curves at constant load for different conditions of sollicitation. The three stages of creep deformation are well described. It is checked that high initial stress levels and high temperatures accelerate the creep process.

NB/In the calculated curves, the same conditions of sollicitation as those of the experimental tests are imposed.

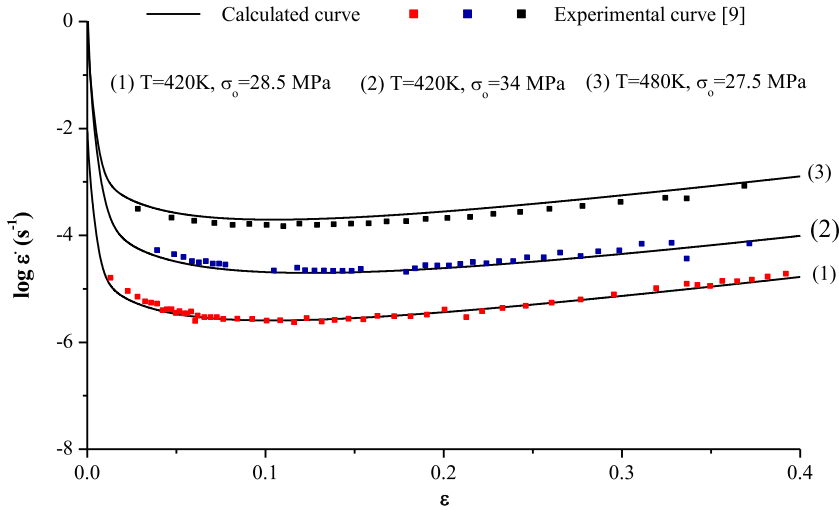


**Figure 1.** Creep curves for Al-1050 sheet under different conditions of sollicitation.

Several experimental works [16, 17] showed that during creep, an abrupt change of the initial stress amplitude ( $\sigma_0$ ) induces a significant change in the material microstructure. Various tests were carried out in this context. At a given temperature ( $T \geq 0.4T_m$ ) and for a defined level of plastic deformation  $\varepsilon^*$ , an abrupt change of  $\sigma_0$  causes a noticeable change in the microstructure via the internal parameters  $\rho$  and  $d$ . The variation in flow stress  $\Delta\sigma$  due to the jump in load between two amounts ( $F_1 = \sigma_{01} \times S_1 \rightarrow F_2 = \sigma_{02} \times S_2$ ) can be determined as follows:

$$\sigma(\varepsilon) = \begin{cases} \sigma_1 = \sigma_{01} \exp(\varepsilon), & \varepsilon < \varepsilon^* \\ \sigma_2 = \sigma_{02} \exp(\varepsilon), & \varepsilon \geq \varepsilon^* \end{cases} \quad (20)$$

$$\Delta\sigma = (\sigma_{02} - \sigma_{01}) \exp \varepsilon^* . \quad (21)$$

According to experimental and numerical works studying the physico-mechanical behaviour of metals, creep test with sudden change in load (or temperature) leads to a rapid change in the material microstructure. This can be explained by the appearance of a transient during the jump: the subgrain size evolves rapidly to reach its new stationary value ( $d_{s2}$ ), while the dislocation density  $\rho$  has a negligible change as long as the deformation is almost constant. For this reason, only the variation of the parameter  $d$  during the jump was considered.

Two steps to consider:

- Just before the jump ( $\varepsilon < \varepsilon^*$ ):

$$\left\{ \begin{array}{l} d_1 = d_{s1} [1 + 2 \exp(-K'_{a1} \varepsilon^*)] \\ \rho_1 = \rho_1^* \end{array} \right\} \quad (22)$$

- Just after the jump ( $\varepsilon > \varepsilon^*$ ):

$$\left\{ \begin{array}{l} d_2 = d_{s2} [1 + 2 \exp(-K'_{a2} \varepsilon^*)] \\ \rho_2 = \rho_2^* \end{array} \right\}, \quad (23)$$

where  $\rho_1^*$  and  $\rho_2^*$  represent the dislocation density just before and after the jump, respectively.

Considering that the dislocation density remains constant during sudden change in load, that is,  $\rho_1^* = \rho_2^*$  and using the relationship (1), we can deduce the physical expression of  $\Delta\sigma$ :

$$\Delta\sigma = \alpha_2 G \sqrt{b} \left( \frac{1}{\sqrt{d_2}} - \frac{1}{\sqrt{d_1}} \right). \quad (24)$$

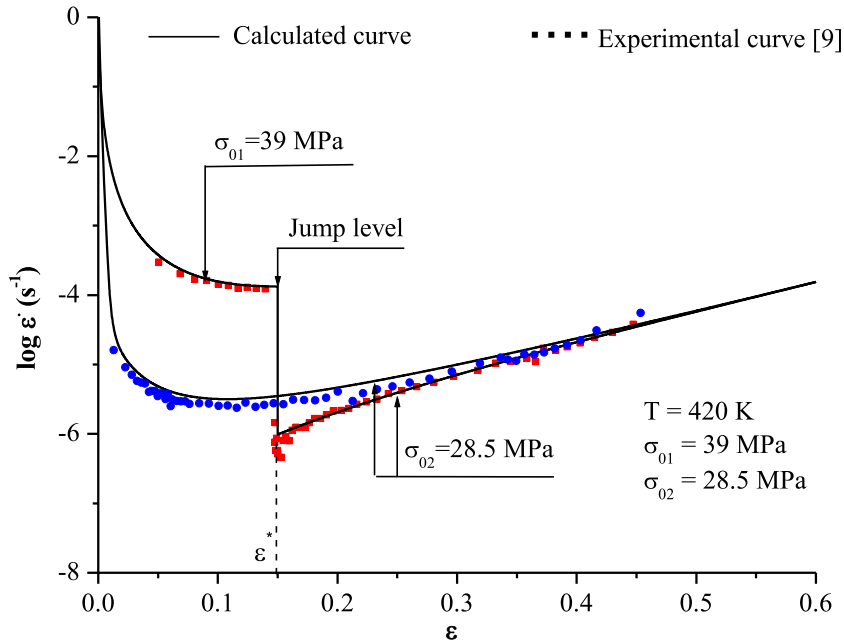


**Figure 2.** Creep test at constant load with a sudden decrease in the load.

In order to simplify the mathematical expression of the relationship (21), we can replace the instantaneous subgrain size by its stationary value  $d_s$ , that is:

- Creep under constant load:

$$d_{s2} = \left[ \frac{(\sigma_{02} - \sigma_{01}) \exp \varepsilon^*}{\alpha_2 G \sqrt{b}} + \left( \frac{1}{d_{s1}} \right)^{\frac{1}{2}} \right]^{-2} \quad (25)$$

- Creep under constant stress:

$$d_{s2} = \left[ \frac{(\sigma_{02} - \sigma_{01})}{\alpha_2 G \sqrt{b}} + \left( \frac{1}{d_{s1}} \right)^{\frac{1}{2}} \right]^{-2} . \quad (26)$$

In order to check the reliability of the proposed model, the calculated results are compared with relevant experimental results in the literature. Two different tests were carried out; one with a sudden decrease in load (Figure 2), while the other is performed by a sudden increase in load (Figure 3). As shown in both figures, a good fit is observed between experimental and calculated curves. These figures show two types of behaviour: continuous creep (without jump) and discontinuous creep (with jump).

After certain period of time, the discontinuous curve tends towards a steady state and converges towards the continuous curve.

Note that, the transient reflect the profound evolution of the internal variable ( $d$ ) that should be progressive (not sudden) between two stationary values  $d_{s1}$  and  $d_{s2}$ . Eventually, the curve after the jump tends towards the steady state and converges towards the curve illustrating the test without the jump. Therefore, we can observe that the abrupt decrease in the load causes a rapid increase in creep rate, while increasing the load causes a rapid decrease in creep rate followed by accelerated growth in its last stage (tertiary creep).

A comparative study was carried out between the two types of creep: at constant load and at constant stress. For this purpose, we have chosen one of the experimental cases available in

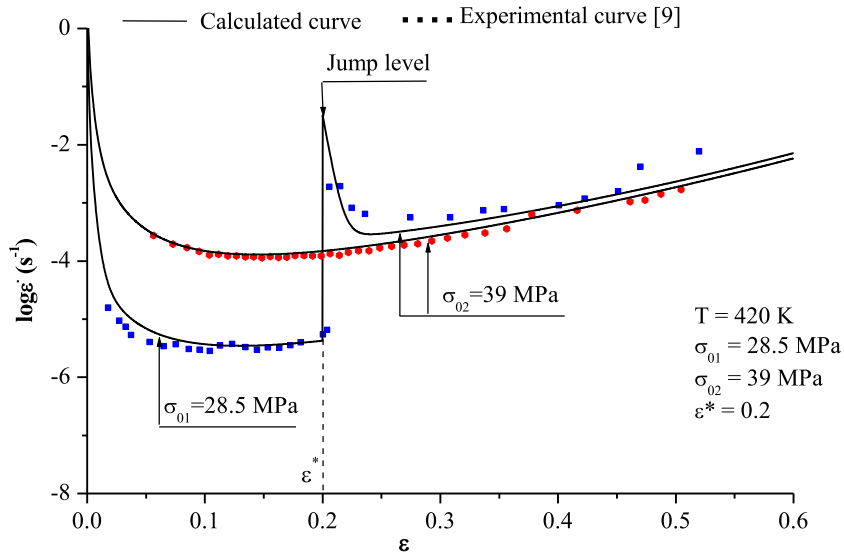


**Figure 3.** Creep test at constant load with a sudden increase in the load.

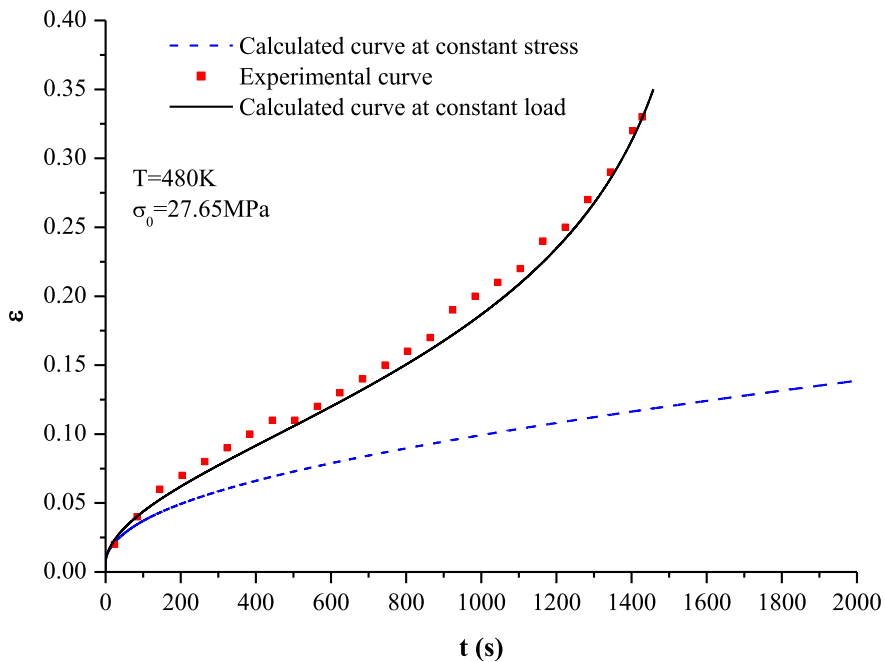


**Figure 4.** Comparison between the creep curve at constant load and creep curve at constant stress.

the literature ( $\sigma_0 = 27.65$  MPa and  $T = 480$  K). Figure 4 illustrates the two types of curves clearly differentiated: in the first case, a significant acceleration of creep in the tertiary stage is observed, this is due to the increased inflow stress, while in the second case, a steady state creep is observed and the tertiary stage has not been reached yet, it indicates a thermomechanical balance between the two simultaneous and antagonistic phenomena: strain hardening and dynamic recovery.



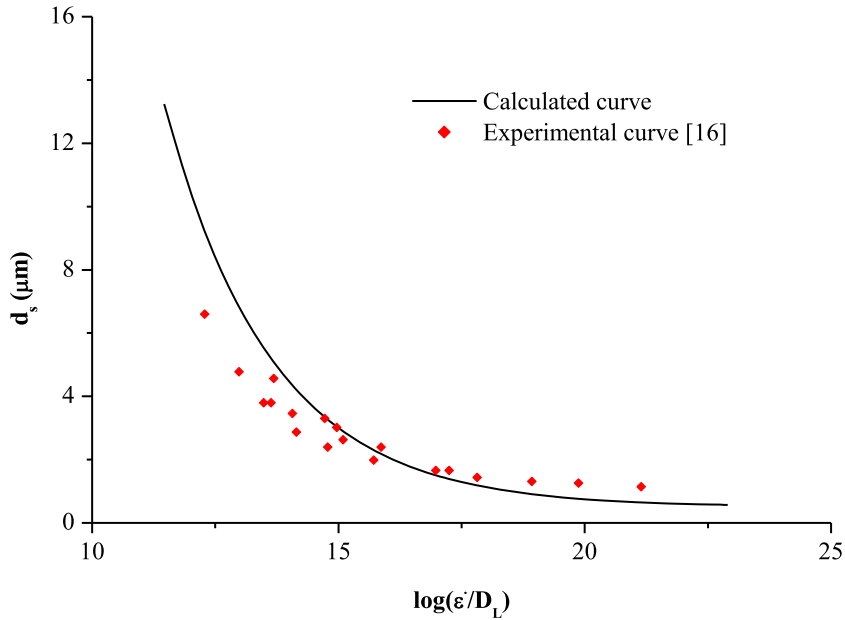


**Figure 5.** Evolution of the subgrain size with temperature and/or strain rate.

Furthermore, the steady state creep behaviour of Al-1050 alloy can be described by (24) derived directly from (1) using the maximum boundary condition:

$$\sigma_s = \alpha_1 G b \sqrt{\rho_s} + \alpha_2 G \sqrt{\frac{b}{d_s}} + \alpha_3 G \sqrt{\frac{b}{D}}. \quad (27)$$

The proposed model still allows us to describe other changes in the material microstructure; for example, Figure 5 shows the evolution of the average subgrain size  $d_s$  as a function of the term  $(\dot{\epsilon}/D_L)$ , which includes the combined effect of strain rate and temperature (replaces the physical parameter of Zener–Hollomon  $Z$ ). The experimental curve is plotted for different values of temperature and strain rate. In the intermediate temperature range ( $293 \text{ K} \leq T \leq 540 \text{ K}$ ), a better agreement is observed between calculated results and experimental data.

#### 4. Conclusion

The proposed study is an extension of preliminary study which has already been published. The encouraging results obtained previously motivated us to develop the proposed model in order to extend it to other complex mechanical behaviour. Understanding response of the material to the combined effect of temperature and strain rate is useful in designing failure resistant systems. Also, understanding the dependence of deformation mechanisms at microscopic scale on the macroscopic material behaviour is more relevant than empirical-based models. The proposed model shows, in a wide range of temperatures and strain rates, the effect of the microstructure parameters on creep behaviour of Al-1050 alloy. This approach can be generalized to metals having FCC crystalline structure. The different figures depict a good agreement between calculated results and experimental data. In addition, this study was carried out on the two types of creep: at constant load and at constant stress. Besides, to assess the reliability of the model, we conducted tests with and without load jump. The study also shows that the flow stress is governed simultaneously by the strain hardening rate ( $\theta$ ) and the strain rate sensitivity ( $\beta$ ). The proposed

methodology has enabled to achieve an adequate description of the thermomechanical response of the material studied during creep tests. Computer programs were carried out to represent the different results.

Finally, this numerical modelling can contribute to simulate several phenomena that result from hot forming, for example, stress relaxation, necking, and thinning behaviour), predict the creep-damage behaviour of metals, extend the study to other types of structure (cc for example) etc.

## Nomenclature

$\sigma$ (MPa)	Applied stress
$F$ (N)	Applied load to the specimen
$S$ (mm <sup>2</sup> )	Specimen cross section
$\theta$ (MPa)	Strain hardening rate
$\beta$	Strain rate sensitivity
$\rho$ ( $\mu\text{m}^{-2}$ )	Dislocation density
$\rho_s$ ( $\mu\text{m}^{-2}$ )	Saturation value of the variable $\rho$
$d$ ( $\mu\text{m}$ )	Subgrain size or dislocation cell size
$d_s$ ( $\mu\text{m}$ )	Saturation value of the variable $d$
$D$ ( $\mu\text{m}$ )	Grain size
$\sigma_\rho$ (MPa)	Internal stress depending on the variable $\rho$
$\sigma_d$ (MPa)	Internal stress depending on the variable $d$
$\sigma_D$ (MPa)	Internal stress depending on the variable $D$
$G$ (MPa)	Shear modulus
$\dot{\epsilon}$ (s <sup>-1</sup> )	Strain rate
$T$ (K)	Deformation temperature
$b$ ( $\mu\text{m}$ )	Burgers vector magnitude
$k_a$	Annihilation factor
$k'_a$	Rate constant
$D_L$ (m <sup>2</sup> ·s <sup>-1</sup> )	Diffusion coefficient
$R$ (J·mol <sup>-1</sup> ·K <sup>-1</sup> )	The gas constant
$T_m$ (K)	Metal melting temperature

## References

- [1] P. Baland, L. Tabourot, M. Fivel, "Comparison of physically based constitutive laws used for numerical simulations of plasticity of metals", *J. Phys. IV* **11** (2001), p. 381-388.
- [2] G. Monnet, L. Vincent, B. Devincre, "Dislocation-dynamics based crystal plasticity law for the low- and high-temperature deformation regimes of bcc crystal", *Acta Mater.* **61** (2013), p. 6178-6190.
- [3] L. Tabourot, A. Maati, P. Baland, M. Vautrot, "Influence of heterogeneities and of their distribution on the elastoplastic", in *International Symposium on Plasticity, Montego Bay, Jamaica*, January 2015.
- [4] E. Nes, "Modelling the evolution in microstructure and properties during plastic deformation of f.c.c metals and alloys — an approach towards a unified model", *Mater. Sci. Eng. A* **322** (2002), no. 1, p. 176-193.
- [5] A. Maati, E. H. Ouakdi, L. Tabourot, P. Baland, M. Demouche, "Modelling of the thermomechanical behaviour of FCC metals under various conditions", *Ann. Chim. Sci. Matér.* **42** (2018), no. 1, p. 115-127.
- [6] F. Zerilli, "Dislocation mechanics-based constitutive equations", *Metall. Mater. Trans.* **35** (2004), p. 2547-2555.
- [7] M. C. Cai, "A constitutive description of the strain rate and temperature effects on the mechanical behaviour of materials", *Mech. Mater.* **42** (2010), p. 774-781.
- [8] H. Fengbo, T. B. Tang, K. Hongchao, L. Jinshan, "Effects of subgrain size and static recrystallization on the mechanical performance of polycrystalline material: a microstructure-based crystal plasticity finite element analysis", *Prog. Nat. Sci.: Mater. Int.* **25** (2015), p. 58-65.

- [9] E. H. Ouakdi, R. Louahdi, G. Ferron, "A physical model describing the viscoplastic behaviour of aluminum under tension and under creep for  $T > 0.4T_m$ ", *J. Mater. Sci. Lett.* **15** (1996), p. 1555-1557.
- [10] J. R. Klepaczko, "Proceedings of the 8th. RISO Int. Symp. on Metallurgy and Materials Science", Riso, Denmark, 1987.
- [11] E. H. Ouakdi, R. Louahdi, "A constitutive model describing the necking behaviour of aluminum during tension and creep", *J. Mater. Sci. Lett.* **17** (1998), p. 193-196.
- [12] H. Luthy, A. K. Miller, O. D. Sherby, "The stress and temperature dependence of steady state flow at intermediate temperatures for pure polycrystalline aluminum", *Acta Metall.* **28** (1980), p. 169-178.
- [13] L. Donghuan, L. Haisheng, L. Yinghua, "Numerical simulation of creep damage and life prediction of superalloy turbine blade", *Math. Probl. Eng.* **1** (2015), p. 1-10.
- [14] T. Furu, R. Orsund, E. Nes, "Subgrain growth in heavily deformed aluminium—experimental investigation and modelling treatment", *Acta Metall. Mater.* **43** (1995), no. 6, p. 2209-2232.
- [15] J. Gil Sevillano, P. van Houtte, E. Aernoudt, "Large strain work hardening and textures", *Prog. Mater. Sci.* **25** (1980), p. 69-134.
- [16] D. M. Dimiduk, "Microstructure-property-design relationships in the simulation era: an introduction", in *Computational Methods for Microstructure-Property Relationships*, Springer, Boston, MA, 2011.
- [17] E. H. Ouakdi, "Modélisation physique du comportement plastique de l'aluminium a moyenne température, application a l'étude de la striction", 1988, Doctoral Thesis, Metz University.